Journal of Steroid Biochemistry and Molecular Biology 242 (2024) 106524

Contents lists available at ScienceDirect

Journal of Steroid Biochemistry and Molecular Biology

journal homepage: www.elsevier.com/locate/jsbmb

Adropin may regulate ovarian functions by improving antioxidant potential in adult mouse

Shweta Maurya [a], Shashank Tripathi [a], Taruna Arora [b], Ajit Singh [a,1,*]

[a] Department of Zoology, Institute of Science, Banaras Hindu University, Varanasi 221005, India
[b] RBMCH Division, ICMR, New Delhi 110029, India

ARTICLE INFO

Keywords:
Adropin
Ovary
hCG
Corpus luteum
Steroidogenesis
Antioxidant

ABSTRACT

The corpus luteum (CL) is a temporary endocrine gland that synthesizes progesterone. The luteal progesterone plays a central role in the regulation of the estrous cycle as well as the implantation and maintenance of pregnancy. Our previous study showed the expression of adropin and its receptor, GPR19, in the luteal cells and its significant role in luteinization. The aim of the present study was to investigate the *in vitro* effect of adropin on hCG-induced ovarian functions in adult mice. We also evaluated the effect of exogenous treatment with adropin on ovarian steroidogenesis and anti-oxidant parameters, with special emphasis on CL function. Our results demonstrated that adropin acts synergistically with hCG to promote ovarian steroidogenesis and survival by increasing the expression of StAR, 3β-HSD, and aromatase proteins and decreasing the BAX/BCL2 ratio. Exogenous adropin treatment increased progesterone production by increasing the expression of GPR19, StAR and 3β-HSD enzymes in the mouse ovary. Also, adropin inhibited the luteal oxidative stress by increasing nuclear translocation of NRF-2 in CL, which resulted in increased HO-1 expression and SOD, catalase activity. Decreased oxidative stress might inhibit the translocation of NF-κB into the nucleus of luteal cells, resulting into increased survival and decreased apoptosis, as evident by decreased lipid peroxidation, BAX/BCL2 ratio, caspase 3, active caspase 3 expression, and TUNEL-positive cells in adropin treated mice. Our findings suggest that adropin can be a promising candidate that can enhance the survivability of the CL.

1. Introduction

Female reproductive functions are under the control of pituitary gonadotropins. These gonadotropins act on the ovary to regulate steroidogenesis and folliculogenesis. The development of follicles is a long process, and increased steroidogenesis during follicular growth leads to enhanced expression of steroidogenic cytochrome P450 enzymes, which is the source of reactive oxygen species (ROS) [1]. Meanwhile, the ovary has a wide range of antioxidant systems that ensure the production of ROS in a controlled manner. The nuclear factor erythroid 2- related factor 2 (NRF-2) and nuclear factor-kappa B (NF-κB) are the two key transcriptional factors that regulate cellular redox homeostasis [2]. Studies revealed that the deletion of NRF-2 in mice leads to a decrease in the number of ovarian follicles, which in turn accelerates ovarian aging [3]. **Luo et al., 2022** reported that a lack of NF-κB signaling promotes the death of granulosa cells, which further causes premature ovarian failure [4]. However, a considerable amount of ROS is required to perform various ovarian activities like folliculogenesis, oocyte maturation, fertilization, and implantation [5]. ROS plays a crucial role in regulating the lifespan of the corpus luteum (CL) and maintaining its

Abbreviations: CL, Corpus Luteum; HCG, human Chorionic Gonadotropin; P4, Progesterone; E2, Estradiol; GPR19, G Protein-coupled Receptor19; ROS, Reactive oxygen species; ELISA, Enzyme-linked immunosorbent assay; SDS-PAGE, Sodium dodecyl sulphate-Polyacrylamide gel electrophoresis; ANOVA, Analysis of Variance; TUNEL, Terminal deoxynucleotidyl transferase dUTP nick end labeling; PVDF, Polyvinylidene fluoride; ECL, Enhanced chemiluminescence, DPX, Dibutylphthalate polystyrene xylene; NRF-2, Nuclear factor erythroid 2- related factor 2; HO-1, Heme oxygenase 1; NF-κB, Nuclear factor- kappa B; StAR, Steroidogenic acute regulatory protein; CYP11A1, Cytochrome p450 11A1; 3β-HSD, 3-beta hydroxy steroid dehydrogenase; SOD, Superoxide dismutase; CAT, Catalase; BCL2, B-cell leukemia/lymphoma 2; BAX, Bcl2 associated X protein.

* Correspondence to: Laboratory No. 4, Reproductive Physiology Laboratory, Department of Zoology, Institute of Science, Banaras Hindu University, Varanasi 221005, India.
E-mail address: ajitsinghrepro@gmail.com (A. Singh).
[1] ORCID- 0000000318493918

https://doi.org/10.1016/j.jsbmb.2024.106524
Received 29 January 2024; Received in revised form 14 March 2024; Accepted 15 April 2024
Available online 24 April 2024

Table 1
List of antibodies that are used for Western blot and immunofluorescence study.

S.No.	Antibody	Host species; Class	Source	Catalogue no.	Dilutions
1	StAR	Rabbit; Polyclonal	Santa Cruz Biotechnology	SC 25806	1:1000 (WB)
2	CYP11A1	Rabbit; Polyclonal	Cell Signaling Technology, Inc.	14217	1:1000 (WB)
3	3β-HSD	Rabbit; Polyclonal	Thermo Fisher Scientific Inc.	PA5–27791	1:800 (WB)
4	Aromatase	Rabbit; Polyclonal	Abcam	ab18995	1:800 (WB)
5	GPR19	Rabbit; Polyclonal	G Biosciences	ITA5843	1:500 (WB)
6	BAX	Rabbit; Polyclonal	Cell Signaling Technology, Inc	2772	1:800 (WB)
7	BCL2	Rabbit; Monoclonal	Cell Signaling Technology, Inc	3498	1:800 (WB)
8	NF-κB p65	Rabbit; Recombinant Polyclonal	Thermo Fisher Scientific Inc.	710048	1:500 (WB) 1:200 (IF)
9	NRF-2	Rabbit; Recombinant Polyclonal	Thermo Fisher Scientific Inc.	710574	1:500 (WB) 1:200 (IF)
10	HO-1	Rabbit; Polyclonal	Cell Signaling Technology, Inc	70081	1:1000 (WB)
11	Caspase 3	Rabbit; Polyclonal	BIOSS	BS-0081R	1:800 (WB)
12	β-Actin	Mouse; Monoclonal HRP-tagged	Sigma Aldrich	A3854	1: 50000 (WB)
13	Rabbit IgG	Goat	GeNei	1140380011730	1:4000 (WB)
14	Alexa Fluor 488 Rabbit IgG	Goat; Polyclonal	Abcam	ab150077	1:300 (IF)

structural and functional integrity throughout the estrous/menstrual cycle [6]. Oxidative stress condition occurs when the equilibrium of ROS and anti-oxidants is disrupted. This affects female reproductive processes and initiates pathological disorders like CL dysfunction, embryonic reabsorption, recurrent pregnancy loss, endometriosis, preeclampsia, and PCOS [5,7–9]. Supplementation with antioxidants has been shown to improve ovarian function by balancing ROS [10].

Adropin, a highly conserved peptide hormone, was identified in 2008 by Kumar and colleagues [11]. The majority of studies have suggested that it plays an important role in the regulation of metabolic homeostasis, mainly glucose and lipid metabolism. Serum adropin level is modulated by body mass index (BMI), diet, and sex [12,13]. The human studies showed the inverse correlation of adropin with BMI [14]. Also, circulating adropin is found to be lower in women than in men [14]. Adropin has been shown to improve hepatic glucose metabolism and insulin sensitivity by suppressing glucose production in HFD mice [15]. Furthermore, adropin also targets muscles and adipose tissue to maintain carbohydrate and fatty acid metabolism. In muscle, adropin activates pyruvate dehydrogenase (PDH) and suppresses carnitine palmitoyltransferase-1B (CPT-1B), indicating that it promotes glucose utilization by enhancing glycolysis [16]. Adropin treatment reduces proadipogenic gene expression and intracellular lipid content during preadipocyte differentiation into mature adipocytes, indicating that it controls white adipogenesis [17]. Apart from the role of adropin in energy homeostasis, this peptide also improves the function of endothelial cells and cardiac metabolism [18–20]. Adropin is reported to be expressed in Leydig cells and improves testicular functions by promoting insulin-stimulated steroidogenesis [21]. Furthermore, recent findings show that adropin enhances NRF-2 transcriptional activity and increases antioxidant responses, thus playing a beneficial role against liver damage [22].

Several peptides that control metabolic response and energy homeostasis have been shown to have a considerable impact on ovarian function, e.g., adiponectin, chemerin, and resistin [23–25]. Since the evidence collectively demonstrated that adropin is an energy homeostasis molecule and exerts a protective role by regulating the NRF2-ROS pathway, we hypothesized that adropin may regulate ovarian function by protecting the gonad from oxidative damage. Therefore, the aim of this study was (a) To elucidate the *in vitro* effect of adropin together with hCG on steroid production; (b) To investigate the effect of exogenous

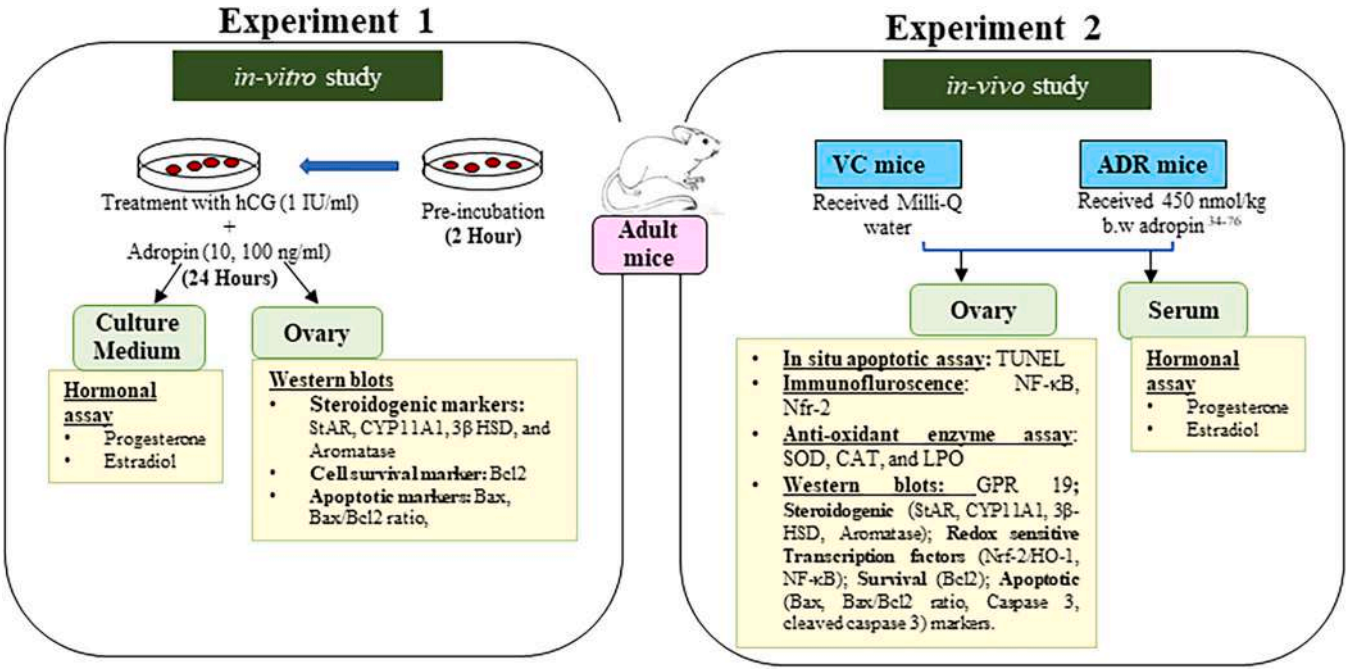

Fig. 1. A schematic diagram illustrating the experimental design for investigating the function of adropin in the ovaries of reproductively active adult mice.

treatment of adropin on steroidogenesis and anti-oxidative parameters in the ovary of adult mice.

2. Materials and method

2.1. Animals

All the experiments were performed in accordance with guidelines adopted by the Committee for Control and Supervision of Experiments on Animals (CPCSEA) and approved by the Institutional Animal Ethical Committee, Institute of Science, Banaras Hindu University, Varanasi, India (BHU/ DoZ/ IAEC/2019–20/034). Female Swiss strain mice were kept in the animal house of the Department of Zoology, Banaras Hindu University, under a standard condition, fed with pelleted food (Mona Laboratory Animal Feeds, Varanasi, India), and water ad *libitum*. Reproductively active adult female mice (12–15 weeks) were used in our experiment. The estrous cycle was tracked using the careful examination of vaginal cytology. Mice that had at least two consecutive regular estrous cycles were chosen for the experiments.

2.2. Peptide

The bioactive adropin peptide (34−36) was purchased from NovoPro Bioscience Inc., Shanghai, China (Catalog: 314322). The lyophilized peptide was reconstituted in Milli-Q water. All general chemicals utilized in this study were purchased from Merck, India. The details of the antibodies are listed in Table 1.

2.3. Experimental design

A schematic diagram of the experimental design is shown in Fig. 1.

2.3.1. Experiment 1: In vitro study

An *in-vitro* study was performed to find out the direct role of adropin together with the hCG on adult mice ovaries (weighing 5-7 mg). Female mice (n = 10/group) were sacrificed in the estrus phase by using mild anesthesia xylazine (8 mg/kg)/ ketamine (60 mg/kg). Ovaries were collected and cleaned in Dulbecco modified Eagle's medium (DMEM; Himedia, Mumbai, India). The ovaries were cultured in a culture medium prepared by the mixing of DMEM and Ham's F12 (1:1; v- v), having penicillin (100 U/ml), streptomycin (100 μg/ml), and 0.1% BSA. The ovaries were initially incubated for 2 h at 37°C. After that, ovaries were cultured with fresh 1 ml of culture medium (supplemented with hCG (1 IU/ml)) without or with different doses of adropin (10 ng/ml (2.223 nmol/liter) and 100 ng/ml(22.23 nmlo/litre) at 37 °C in a humidified atmosphere with 95% air and 5% CO_2 for 24 hours. The experiment was repeated three times. In the end, the ovaries were collected, PBS-washed, and stored at −20°C for a Western blot study. The media were also kept at −20 °C for steroid hormone assay. Doses of adropin were selected on the basis of previous studies [26,27].

2.3.2. Experiment 2: In vivo study

In vivo study was performed to examine the effect of adropin on ovarian function. For this, the reproductively active adult females (12–15 weeks; 28–30 gm b.w.) mice were divided into two groups (n= 10/group). The vehicle control (VC) group mice were injected with vehicle, i.e., Milli-Q water only. Whereas, adropin-treated (ADR) group mice were administered with 450 nmol/kg body weight adropin. Mice were fasted overnight before starting the experiment. Vaginal cytology was examined, and doses were given in the estrus phase of the estrous cycle. The three intraperitoneal injections of adropin were given at the interval of 6 hours. The mice were sacrificed after two hours of the last injection by mild anesthesia xylazine (8 mg/kg)/ketamine (60 mg/kg). Ovaries were excised and cleaned from any adherent fat bodies. Five ovaries of each group (one from each mouse) were fixed in Bouin's fixative for histological examination. The rest of the ovaries were kept at −20 °C for immunoblots. The serum was isolated from the blood and kept at −20 °C for steroid hormones assay. Doses of adropin and administration protocol were chosen based on prior studies [16,28].

2.4. Histological analysis

Bouin's fixed ovaries were dehydrated with different grades of ethanol, cleared with xylene, and embedded in paraffin wax. Ovaries were serially sectioned at 6 μm with a microtome and spread on poly L-lysine coated slides. Further, these slides were processed for hematoxylin-eosin and immunofluorescence staining.

2.5. Immunofluorescence (IF) detection of NRF-2 and NF-κB

Ovarian sections were deparaffinized in xylene, hydrated in descending grades of alcohol, and washed with 0.1 M PBS (pH 7.4). Antigen retrieval was performed by microwave heating at 750 W in 10 mM citrate buffer (pH 6.0) for 10 min. The sections were washed thrice with 0.1 M PBS for 5 min each, followed by the blocking of endogenous peroxidase activity with 3% H_2O_2 in methanol for 20 min. After washing with 0.1 M PBS, sections were incubated with blocking serum for 2 hours, followed by overnight incubation with a primary antibody. Afterward, sections were washed thrice with 0.1 M PBS for 10 min each, followed by 2 hours of incubation with Alexa Fluor 488 goat anti-rabbit secondary antibody at room temperature in a dark chamber. The slides were again washed with 0.1 M PBS, mounted with DABCO, and visualized with a laser scanning super-resolution microscope (Leica, Germany). The quantitation of immunostaining was performed using Zen microscopy software version 3.9 (Zeiss) to calculate the mean intensity value of the fluorescent signals at ten randomly selected nuclei/cytoplasmic areas in each image.

2.6. Immunoblot

10% ovarian homogenate was prepared from pooled ovarian samples in a suspension buffer (0.01 M Tris pH 7.6, 0.001 M EDTA pH 8.0, 0.1 M NaCl, 1 μg/ml aprotinin, 100 μg/ml PMSF). Protein isolation and Western blotting were carried out as described previously by Maurya & Singh, 2022 [29]. The total protein content was determined by the Bradford method [30]. After that, an equal amount of proteins (60 μg) were run on 12% SDS-PAGE gel. The separated proteins were electrophoretically transferred from gel to PVDF membrane overnight at 50 volts, 4°C. After confirming the transfer efficiency of protein by Ponceau- S, the membrane was blocked with phosphate-buffered saline (0.01 M, pH 7.4; NaH_2PO_4 16 mM, Na_2HPO_4 64 mM, NaCl 154 mM, 0.02% Tween 20) containing 5% fat-free milk for 1 h followed by 3 h incubation with primary antibody. Thereafter, membrane was washed thrice (10 minutes each) with PBS-Tween20 and then incubated with a secondary antibody for 2 h. Afterward, the membrane was washed again with PBS- Tween 20 for three times (10 minutes each), followed by signal development by using enhanced chemiluminescence (ECL) detection kit (Biorad, USA) on X-ray film. The resulting bands were analyzed and quantified by Image- J software (Image J, USA).

2.7. Serum hormone assay: progesterone (P4) and Estradiol (E2)

ELISA kits for the measurement of P4 and E2 were purchased from Diametra (Lot no. DKO006/DKO003), and experiments were performed as per the manufacturer's protocols. For the assay, 20 μl and 25 μl of standard or sample were added in each well of P4 and E2 ELISA plate, respectively, followed by the addition of 200 μl of enzyme conjugate solution. Then, P4 and E2 ELISA plates were incubated at 37°C for around 1 h and 2 h, respectively. After that, contents were removed from each well and washed thrice with wash buffer. Then, 100 μl tetramethyl benzidine solution was added to each well, and P4 and E2 ELISA plates were kept in a dark chamber for 15 and 30 minutes,

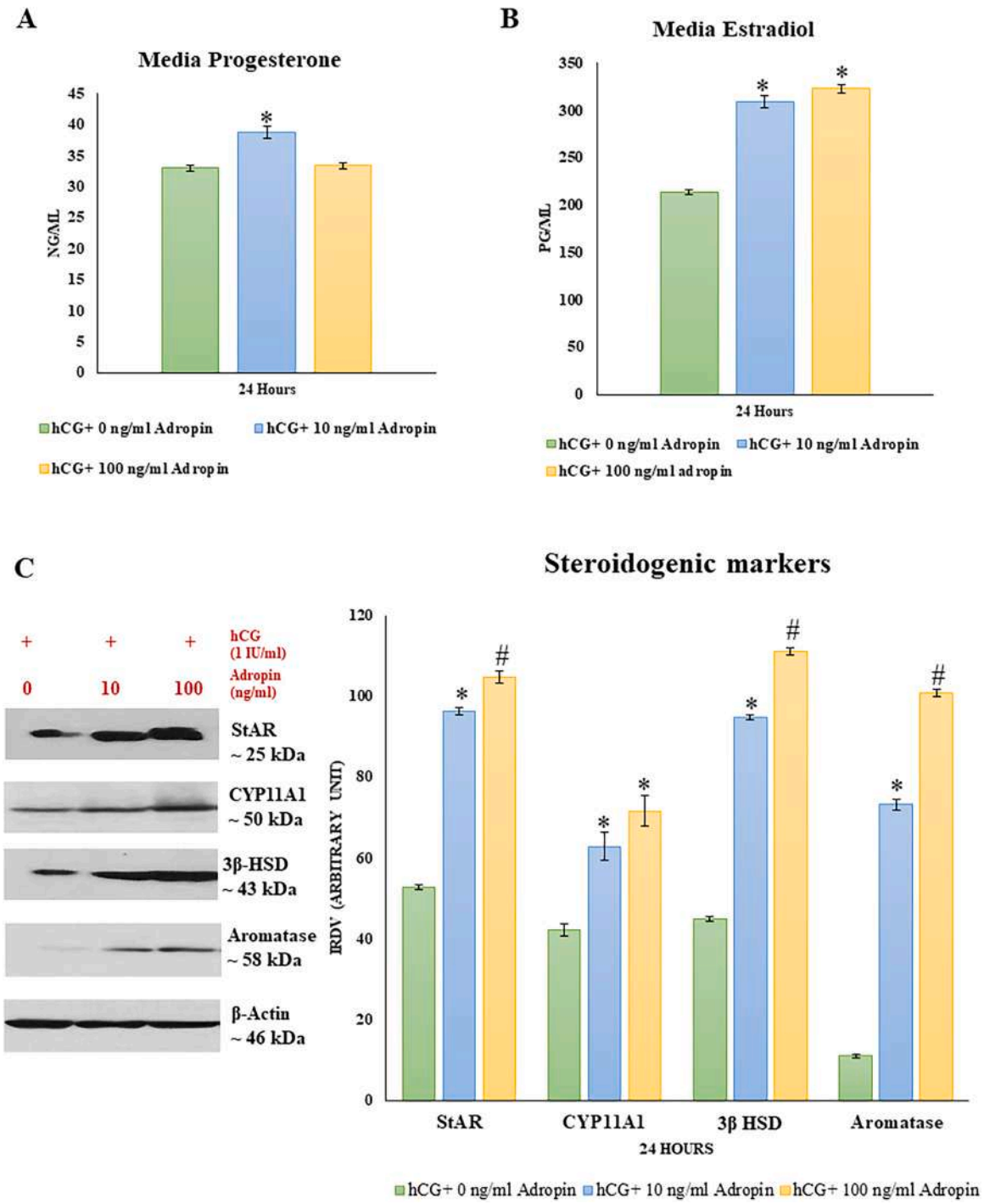

Fig. 2. Effect of *in vitro* treatment of adropin (10 and 100 ng/ml) supplemented with hCG (1 IU/ml) on (A) media progesterone and (B) media estradiol concentrations. (C) Representative immunoblots and densitometric analysis of steroidogenic proteins, namely steroidogenic acute regulatory protein (StAR), CYP11A1, 3β-hydroxysteroid dehydrogenase (3β-HSD), and aromatase in mice ovary treated with adropin (10, 100 ng/ml) together with hCG. Data are represented as mean or IRDV±SEM (n=3), analyzed by one-way ANOVA followed by the post-hoc Bonferroni test. A bar with distinct superscript (*, #) denoted that there is a significant difference ($p<0.05$) between the mean values. β-actin is used to normalize the results of immunoblots. IRDV, Integrated relative density value.

respectively. Finally, 100 µl of 0.2 M sulphuric acid was added to stop the reaction, and absorbance was taken at 450 nm.

2.8. Evaluation of antioxidant enzyme activities

The activity of superoxide dismutase (SOD), catalase (CAT), and level of lipid peroxidation (LPO) was measured in the ovary. Ovary was pooled, and homogenate (10% w/v) was prepared in ice-cold PBS (0.01 M, pH 7.6). Then, the homogenate was centrifuged at 12000 g at 4°C for 30 min, and the supernatant was collected. Ovarian protein content was estimated by the Bradford method.

2.8.1. SOD activity assay

The SOD activity was determined according to **Das et al., 2000** [31]. The 100 µl of processed supernatant was treated with 1.4 ml of reaction mixture [1.1 ml PBS (50 mM) pH 7.6, 80µl $_L$-Methionine (20 mM), 80 µl

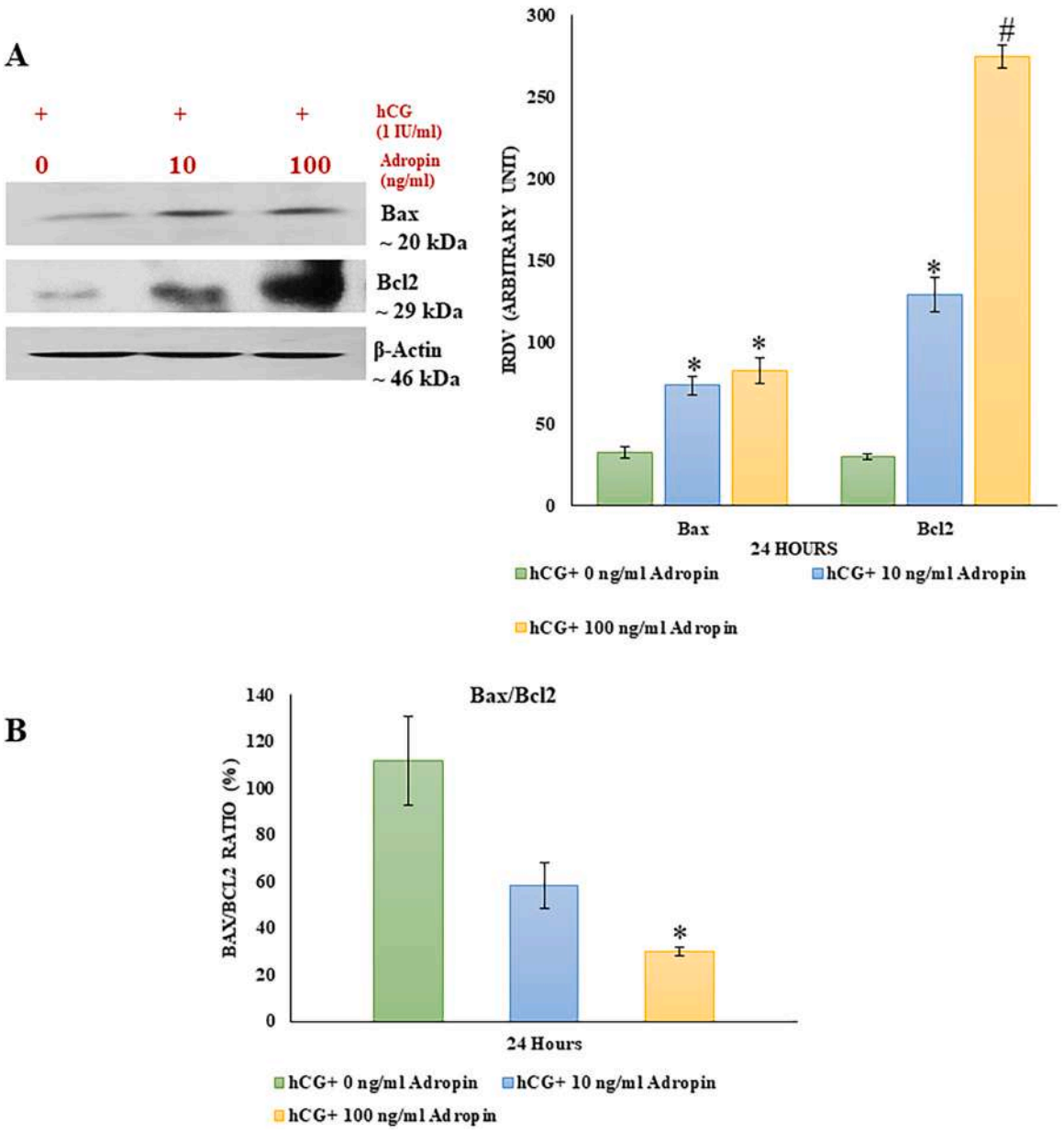

Fig. 3. Representative immunoblots and densitometric analysis of (A) BAX and BCL2 proteins in adropin-treated ovaries (10, 100 ng/ml) supplemented with hCG (1 IU/ml) for 24 hours. (B) The bar graph represents the BAX/BCL2 ratio (in %) in hCG- induced adropin treated adult mice ovary. Data are expressed as IRDV±SEM (n= 3), analyzed by one-way ANOVA followed by the post-hoc Bonferroni test. A bar with distinct superscript (*, #) denoted that there is a significant difference ($p<0.05$) between the mean values. β-actin is used to normalize the results of immunoblots. IRDV, Integrated relative density value.

hydroxylamine hydrochloride (10 mM), 40 µl Triton-x-100 (1% v/v)] and incubated for 5 min at 37°C. Thereafter, 80 µl of Riboflavin (50 µM) was added to each sample in red light and kept in SOD illuminated light box for 10 min. Finally, 1 ml of freshly prepared Griess reagent (1% sulphanilamide, 5% orthophosphoric acid, 0.1% N-(1- napthyl) ethyl-enediamine dihydrochloride) was added to each sample tube and absorbance was taken at 543 nm by using a multimode microplate reader (Synergy H1; Biotek Instruments, Winooski, VT, USA). Enzyme activity was expressed as units (U)/mg of proteins.

2.8.2. CAT activity assay

The CAT activity in ovarian tissue was estimated according to Sinha, 1972 [32]. The 1 ml of supernatant was added to the mixture of 4 ml H_2O_2 (0.8 M) and 5 ml PBS (0.01 M). Then, this mixture was incubated for 1 min. After that, an aliquot of 1 ml from the above mixture was taken, and 2 ml of acidic potassium dichromate solution was added. This final mixture was incubated for 10 min in the hot water bath (95°C). After cooling, the absorbance was noted at 570 nm using a multimode microplate reader (Synergy H1; Biotek Instruments, Winooski, VT, USA). The activity of CAT was represented as the amount of H_2O_2 depleted/min/mg of protein.

2.8.3. LPO assay

Lipid peroxidation (LPO) was estimated according to Ohkawa et al., 1978 [33]. The 0.2 ml of supernatant was mixed with 3.3 ml of thio-barbituric acid (TBA) reagent [0.2 ml sodium dodecyl sulphate (8%), 1.5 ml acetic acid (20%) at pH 3.5, 1.5 ml TBA (0.8%), 0.1 ml butylated hydroxyl toluene (0.8%)] and incubated for 1 h in the hot water bath (95°C). Thereafter, the reaction mixture was cooled and centrifuged at 500 x g for 10 min at 4°C. The supernatant containing malonaldehyde (MDA)-TBA byproduct was measured at 532 nm using a multimode microplate reader (Synergy H1; Biotek Instruments, USA).

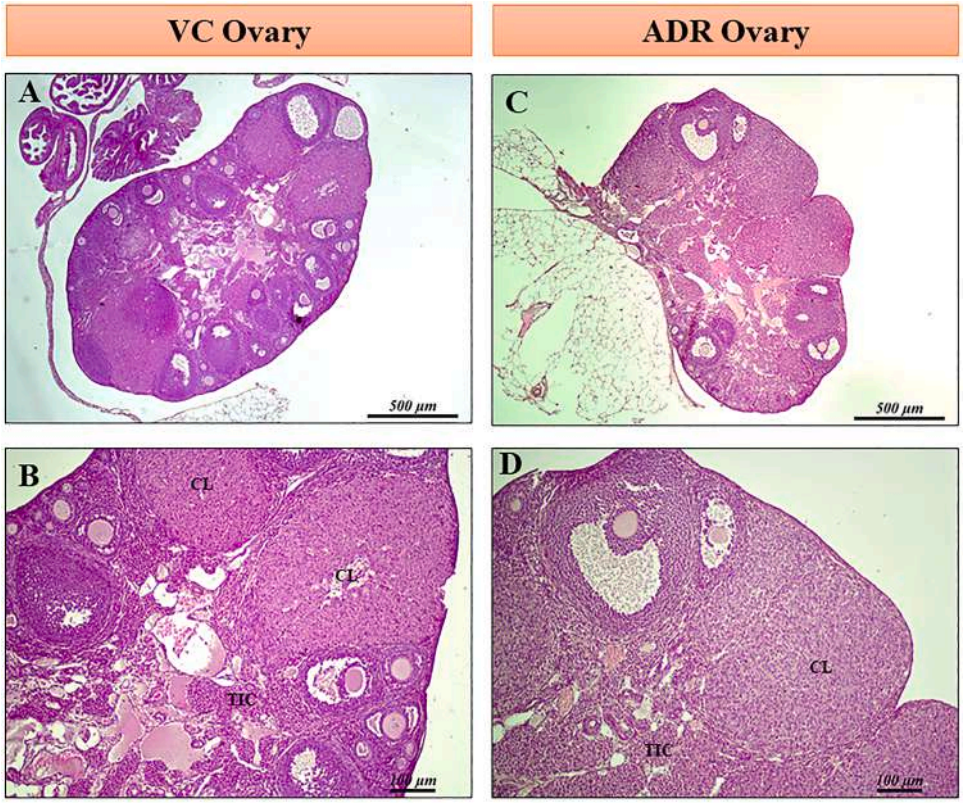

Fig. 4. Representative images of ovaries (stained with hematoxylin-eosin) of reproductively active adult mice are showing no histological changes after the exogenous treatment of adropin (450 nmol/kg b.w.). (A-B) Ovary of VC mice; (C-D) Ovary of ADR mice. Figs. A and C are shown in 4x magnification, whereas Figs. B and D are shown in 10x magnification. Abbreviations: CL- Corpus luteum; TIC- theca interstitial cells; VC- vehicle control; ADR- adropin treated group (450 nmol/kg b.w.).

2.9. Terminal deoxynucleotidyl transferase-mediated dUTP nick end labeling (TUNEL) assay

TUNEL assay was performed in the paraffin section by using Elabscience TUNEL in situ apoptosis kit (catalog no: E-CK-A331, Elabscience Biotechnology Inc., Texas, USA) according to the manufacturer's protocol. Briefly, ovarian sections were deparaffinized in xylene, hydrated in graded ethanol (absolute, 90%, 70%, 50%), washed in 0.1 M PBS, and incubated in proteinase K at 37 °C for 20 min. Then, the sections were washed with 0.1 M PBS for three times of 5 min each and immersed in a blocking buffer (3% hydrogen peroxide in methanol) at room temperature for 20 min. Sections were initially incubated in TdT equilibration buffer at 37 °C for 20 min, followed by incubation in 50 µl TdT enzyme working solution (40 µl TdT equilibration buffer, 5 µl Biotin-dUTP, 5 µl TdT enzyme) at 37 °C for 1 h with shaded light in a humidified chamber. After rinsing with 0.1 M PBS, the sections were incubated in 100 µl streptavidin-HRP working solution at 37 °C for 30 min with shaded light in a humidified chamber. The sections were again washed with 0.1 M PBS and incubated with 3, 3'- diaminobenzidine (DAB) solution for 1–5 min. After rinsing with 0.1 M PBS, the sections were counterstained with hematoxylin staining solution, dehydrated in graded ethanol (70%, 90%, and absolute) for 10 min each, cleared in xylene, and mounted with Dibutylphthalate Polystyrene Xylene (DPX). The apoptotic cells were observed and photographed under a light microscope (Nikon, Tokyo, Japan).

2.10. Statistical analysis

All the statistical analyses were performed using SPSS version 16 software (SPSS Inc, IBM, Chicago, IL, USA). The significance of mean values among hCG-supplemented adropin-treated groups (10, 100 ng/ml) was determined by one-way ANOVA followed by the post-hoc Bonferroni test. The mean values of VC and ADR mice were compared using an unpaired t-test. Data were presented as mean± SEM, while densitometric data were expressed as the mean of integrated relative density value (IRDV) ±SEM. The data were considered statistically significant if $p<0.05$.

3. Results

3.1. Experiment 1: effect of in vitro treatment of adropin (ADR) together with hCG on adult mice ovary

3.1.1. Changes in media steroid concentration and expression of steroidogenic markers in the ovary

The culture of adult mice ovary with ADR along with hCG showed a significant increase in P4 level ($p= 0.004$) at 10 ng/ml, while no change was recorded at 100 ng/ml ADR dose in comparison with the VC (Fig. 2A). On the other hand, both the ADR doses showed a significant ($p<0.001$) increase in media E2 concentration as compared to the VC (Fig. 2B). The effect of different doses of ADR in hCG-stimulated ovarian culture showed a dose-dependent significant ($p<0.001$) increase in the expression of StAR, 3β-HSD, and aromatase protein as compared to the VC. A significant increase was noted in CYP11A1 expression at both 10 ng/ml ($p=0.010$) and 100 ng/ml ($p= 0.002$) doses of ADR in comparison with the VC (Fig. 2C).

3.1.2. Changes in the expression of pro- and anti-apoptotic markers expression in the ovary

The effect of *in vitro* treatment of ADR on the ovarian expression of BAX and BCL2 in the mice is shown in Fig. 3. Densitometric analysis of immunoblot of BCL2 (anti-apoptotic) protein showed a significant ($p<$

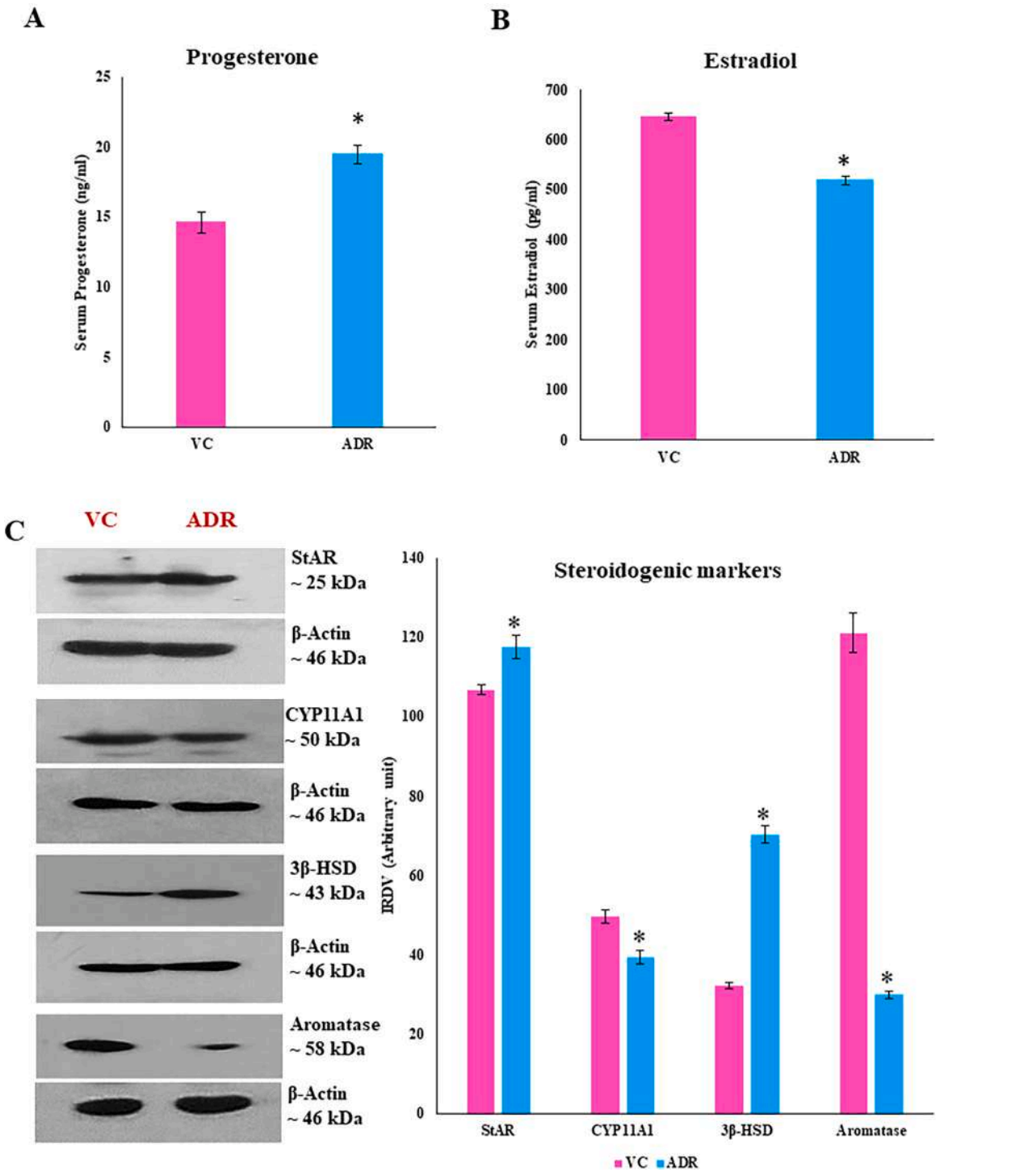

Fig. 5. Effect of adropin treatment (450 nmol/kg b.w.) on circulating (A) progesterone and (B) estradiol concentration in adult mice. (C) Representative immunoblots and densitometric analysis of ovarian steroidogenic proteins, namely steroidogenic acute regulatory protein (StAR), cytochrome P450 side chain cleavage enzyme (CYP11A1), 3β-hydroxysteroid dehydrogenase (3β-HSD), and aromatase in VC and ADR mice. Data are expressed as mean or IRDV ±SEM (n=3), analyzed by unpaired t-test. A bar with a (*) superscript indicates a statistically significant ($p<0.05$) difference between the mean values of VC and ADR. β-actin is used to normalize the results of immunoblots. IRDV, integrated relative density value; VC, Vehicle control; ADR, adropin-treated group.

0.001) dose-dependent increase in ADR ovary as compared to VC. We also found a significant increase in BAX (pro-apoptotic) protein expression at both doses of ADR as compared with the VC (Fig. 3A). However, the ratio of BAX/BCL2 protein was noted to be significantly declined at 100 ng/ml (p= 0.010) ADR dose as compared to the VC (Fig. 3B).

3.2. Experiment 2: effect of intraperitoneal administration of adropin (ADR) in the mice- in vivo study

3.2.1. Changes in the ovarian histology

The mice treated with exogenous ADR showed no marked histo-architecture variations in the ovary (Fig. 4).

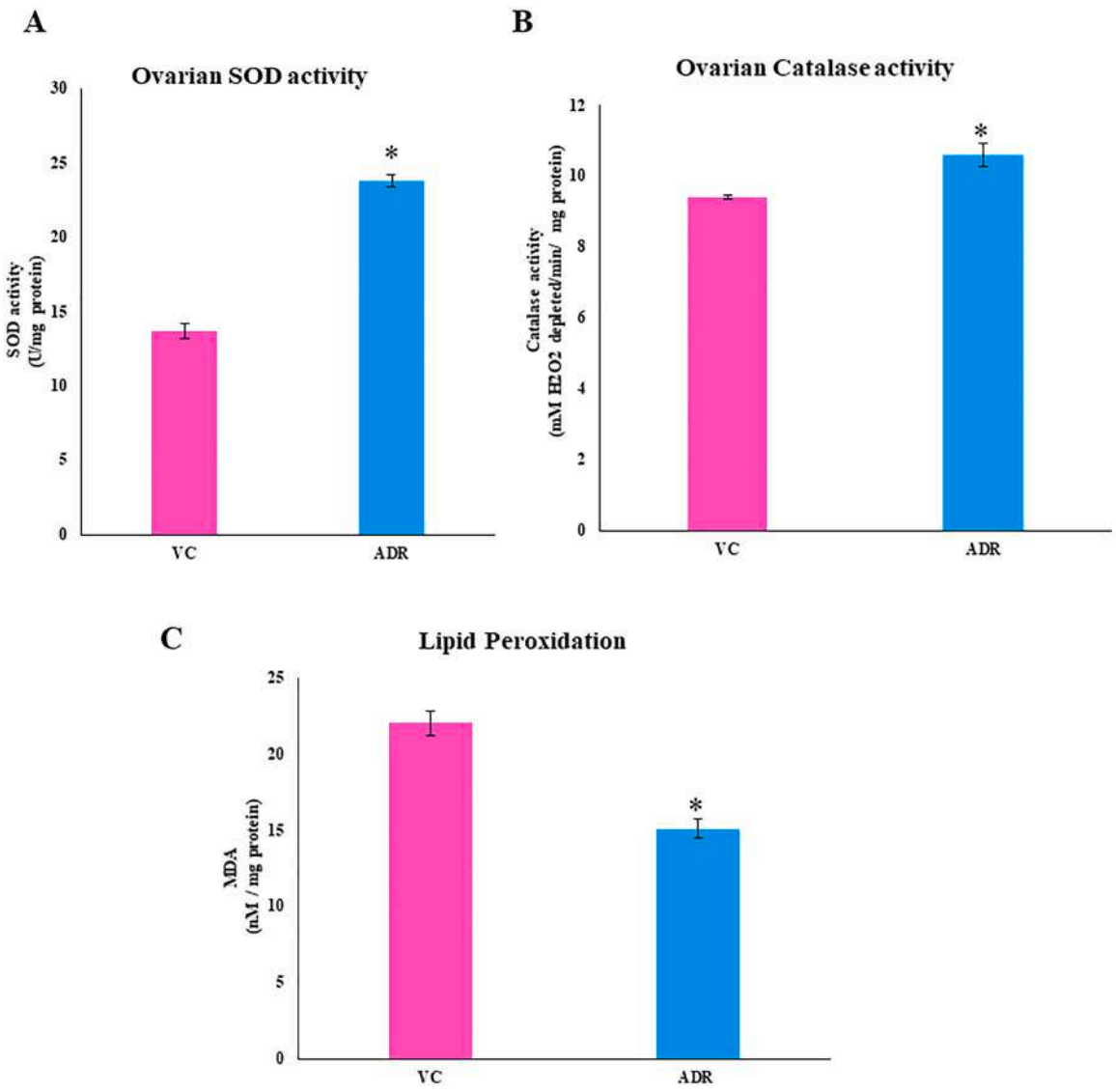

Fig. 6. Effect of exogenous administration of adropin (450 nmol/kg b.w.) on ovarian antioxidant status (A) superoxide dismutase (SOD) activity, (B) catalase activity, (C) lipid peroxidation level in reproductively active adult mice. Data are expressed as mean ±SEM (n=3). A bar with a (*) superscript indicates a statistically significant ($p<0.05$) difference between the mean values of VC and ADR groups. VC, Vehicle control; ADR, adropin-treated group.

3.2.2. Circulating steroid level and ovarian expression of steroidogenic markers

The intraperitoneal treatment of ADR (450 nmol/kg body weight) showed a significant increase in serum P4 ($p= 0.008$; Fig. 5A) while E2 ($p<0.001$; Fig. 5B) concentration was significantly decreased as compared to the VC. Densitometric analysis of steroidogenic enzymes showed a marked variation in ADR mice ovary (Fig. 5C). A significant increase was noted in the expression of StAR ($p= 0.028$) and 3β-HSD ($p<0.001$), while a significant decrease was observed in the ovarian expression of CYP11A1 ($p= 0.004$) and aromatase ($p<0.001$) in the ovary of ADR group as compared to the VC.

3.2.3. Ovarian antioxidant enzyme activity and lipid peroxidation

A significant rise in the activity of SOD ($p<0.001$; Fig. 6A) and CAT ($p= 0.023$; Fig. 6B) was noted in the ovary of ADR mice as compared to the VC. On the other hand, the level of lipid peroxidation (MDA content) was found to be significantly ($p= 0.002$) decreased in the ovary of ADR with respect to the VC (Fig. 6C).

3.2.4. Ovarian expression of GPR19, NF-κB, NRF-2, HO-1, BAX, BCL-2, caspase 3 proteins and TUNEL positive cells

Densitometric analysis of Western blot revealed a significant increase in expression of GPR19 ($p<0.001$; Fig. 7A), NF-κB ($p<0.001$; Fig. 7B), NRF-2 ($p= 0.020$; Fig. 7C), HO-1($p<0.001$; Fig. 7C) and BCL2 ($p<0.001$; Fig. 9A) in the ovary of ADR mice in comparison to the VC. On the other hand, a significant reduction ($p<0.001$) in the ovarian expression of BAX (Fig. 9A), caspase 3 (Fig. 9B), and cleaved caspase 3 (Fig. 9B) protein was noticed in the ADR group with respect to the VC. It was also observed that the ratio of BAX/BCL2 significantly ($p<0.001$) decreased in the ADR group as compared to the VC group (Fig. 9C). Further, apoptosis was assessed by performing the TUNEL assay. Positive signals were detected in the nucleus of apoptotic cells. We observed more TUNEL-positive signals in the luteal cells of the ovary of VC mice. However, very few or no TUNEL-positive cells were seen in the CL of the ADR ovary (Fig. 8A and B).

3.2.5. Immunofluorescence detection of NF-κB and NRF-2 proteins

The immunofluorescence visualization of NF-κB protein showed its distinct localization in luteal cells of VC and ADR ovary. In the VC ovary, NF-κB protein was detected in the nuclei of luteal cells, also we observed

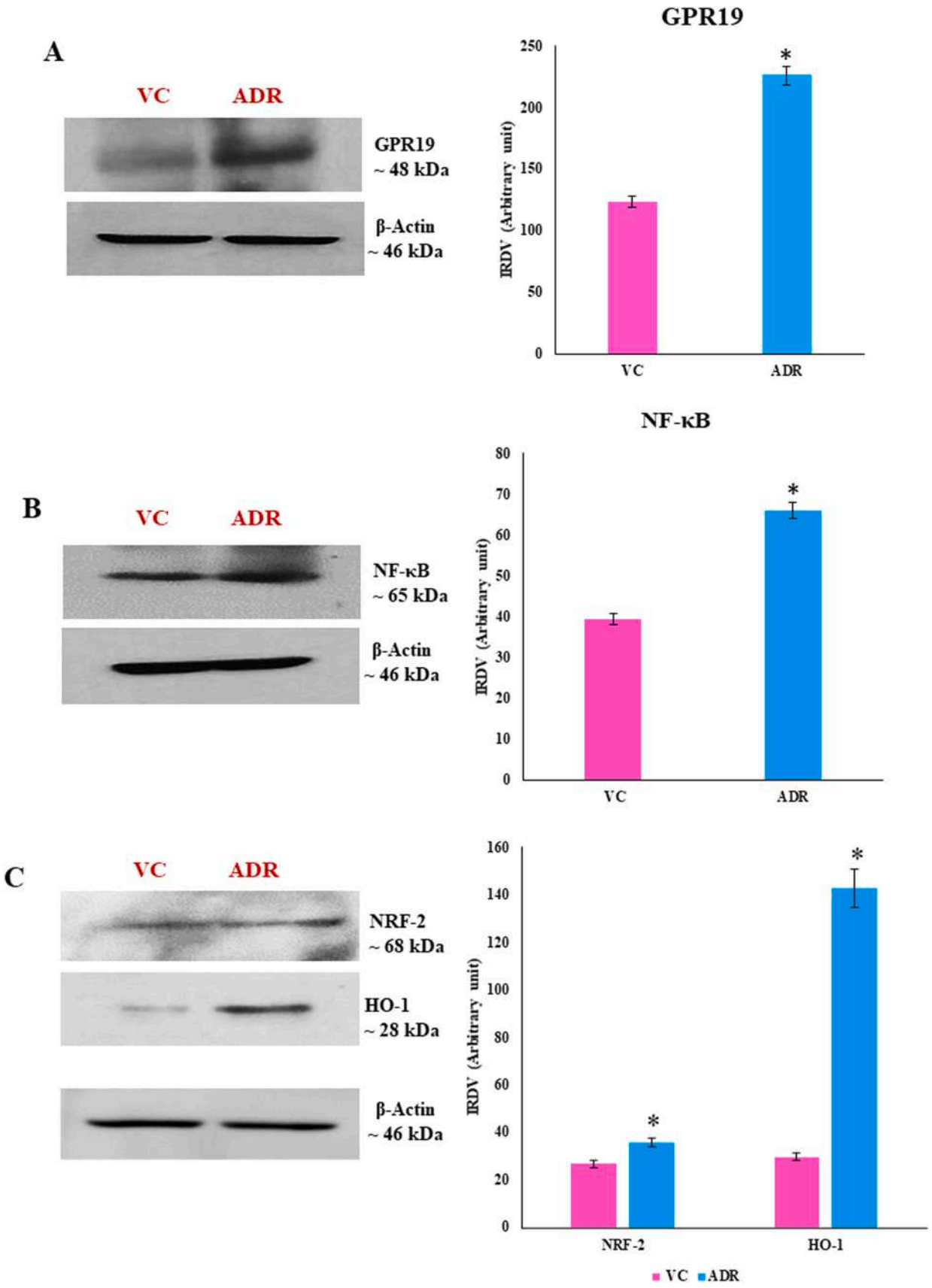

Fig. 7. Representative immunoblots and densitometric analysis of ovarian (A) GPR19, (B) NF-κB, (C) NRF-2 and HO-1 proteins in adult VC and ADR mice. Data are expressed as IRDV ± SEM (n=3), analyzed by unpaired t-test. A bar with a (*) superscript indicates a statistically significant ($p<0.05$) difference between the mean values of VC and ADR groups. VC, Vehicle control; ADR, adropin-treated (450 nmol/kg b.w.) group.

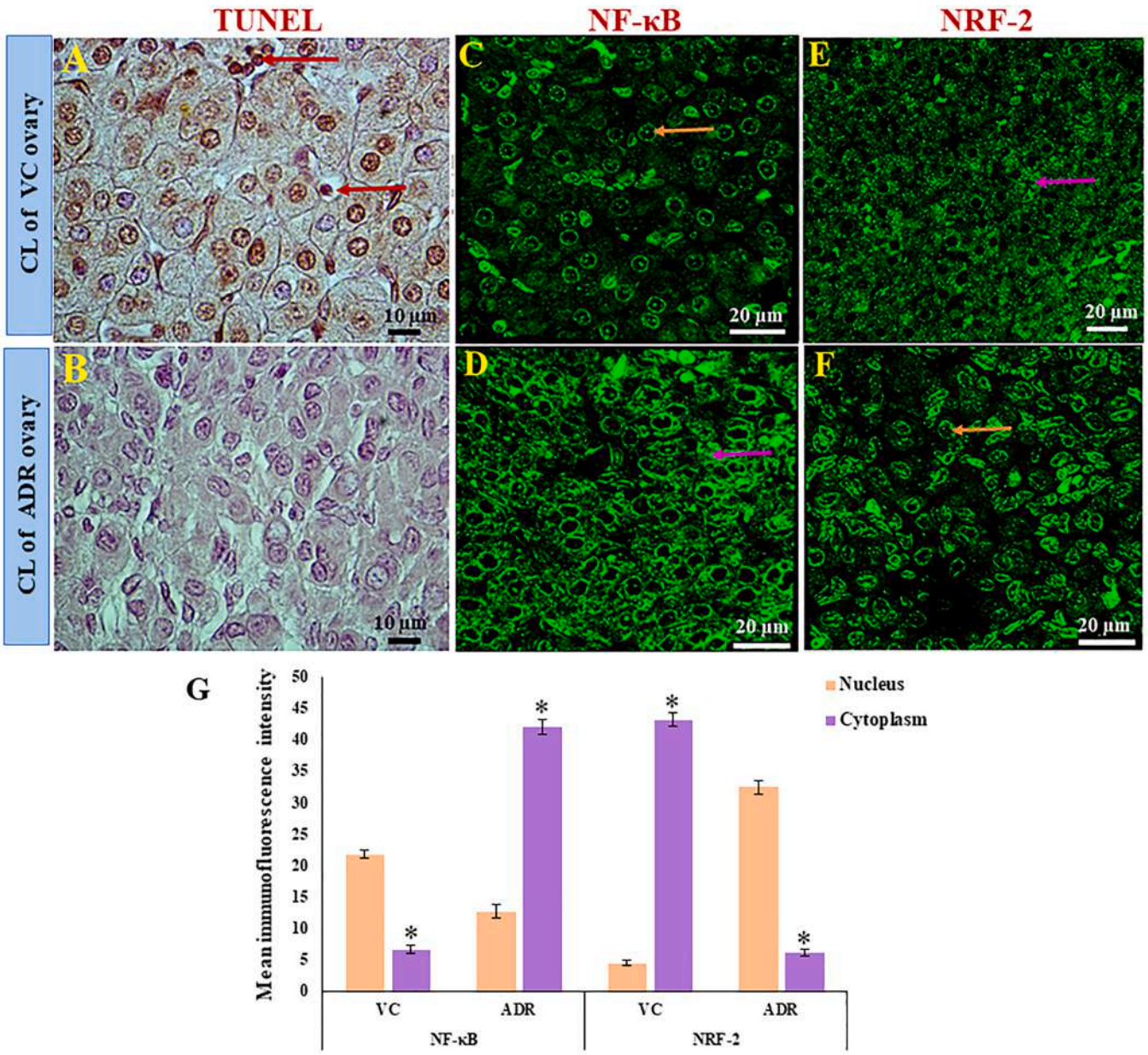

Fig. 8. (A-B) TUNEL assay and immunofluorescence detection of (C-D) NF-κB and (E-F) NRF-2 proteins in the paraffin-embedded sections of the ovary of adult mice treated with adropin (450 nmol/kg b.w.). (G) Quantitation of the immunostaining of NF-κB and NRF-2 in the nucleus and cytoplasm of luteal cells. Bars represents mean ± SEM. (A, C, E) corpus luteum of VC mice ovary; (B, D, F) corpus luteum of the ADR mice ovary. Scale bar: 10 µm (A-B) and 20 µm (C-F). Red arrow shows apoptotic cell, orange arrow shows nucleus, pink arrow shows cytoplasm. (*) symbol indicates a statistically significant ($p<0.05$) difference between the mean values of nucleus and cytoplasm of luteal cells.

significantly ($p<0.001$) high fluorescent signals in the nucleus as compared to the cytoplasm of the luteal cell. Moreover, the CL of the ADR ovary showed a shift in localization from the nucleus to the cytoplasm of the luteal cells (Fig. 8C and D). As a result, we noted significantly ($p<0.001$) high fluorescent signals in the cytoplasm as compared to the nuclei of the luteal cells (Fig. 8G). However, the localization of NRF-2 in the luteal cells of VC and ADR ovaries differed. The presence of NRF-2 was restricted mainly in the cytoplasm of luteal cells in VC as we observed significantly ($p<0.001$) high fluorescent intensity in the luteal cytoplasm as compared to the nuclei of the CL. In contrast, the quantification of the immunofluorescence study showed the high fluorescent intensity of NRF-2 in the nuclei as compared to the cytoplasm of luteal cells in the CL of ADR ovary (Fig. 8E-G).

3.2.6. *Correlation analysis*

The statistical relationship between GPR19 and various oxidative stress parameters was assessed by performing Pearson's correlation. We noticed a significant positive correlation of GPR19 with the ovarian SOD ($r = 0.988$) and CAT ($r = 0.874$) activities, whereas a negative correlation was found with the LPO ($r = -0.960$). Furthermore, changes in the integrated relative density value (IRDV) of GPR19 immunoblot was correlated with the circulating P4 and IRDV of 3β-HSD, NRF-2, HO-1, BAX, BCL2, and cleaved caspase 3 proteins. GPR19 showed a significant positive correlation with the serum P4($r = 0.882$), 3β-HSD ($r = 0.967$), NRF-2 ($r = 0.822$), HO-1 ($r = 0.954$), and BCL2 ($r = 0.949$) proteins, while negative correlation with the BAX protein ($r = -0.989$) and cleaved caspase 3 ($r = -0.990$) (Table 2).

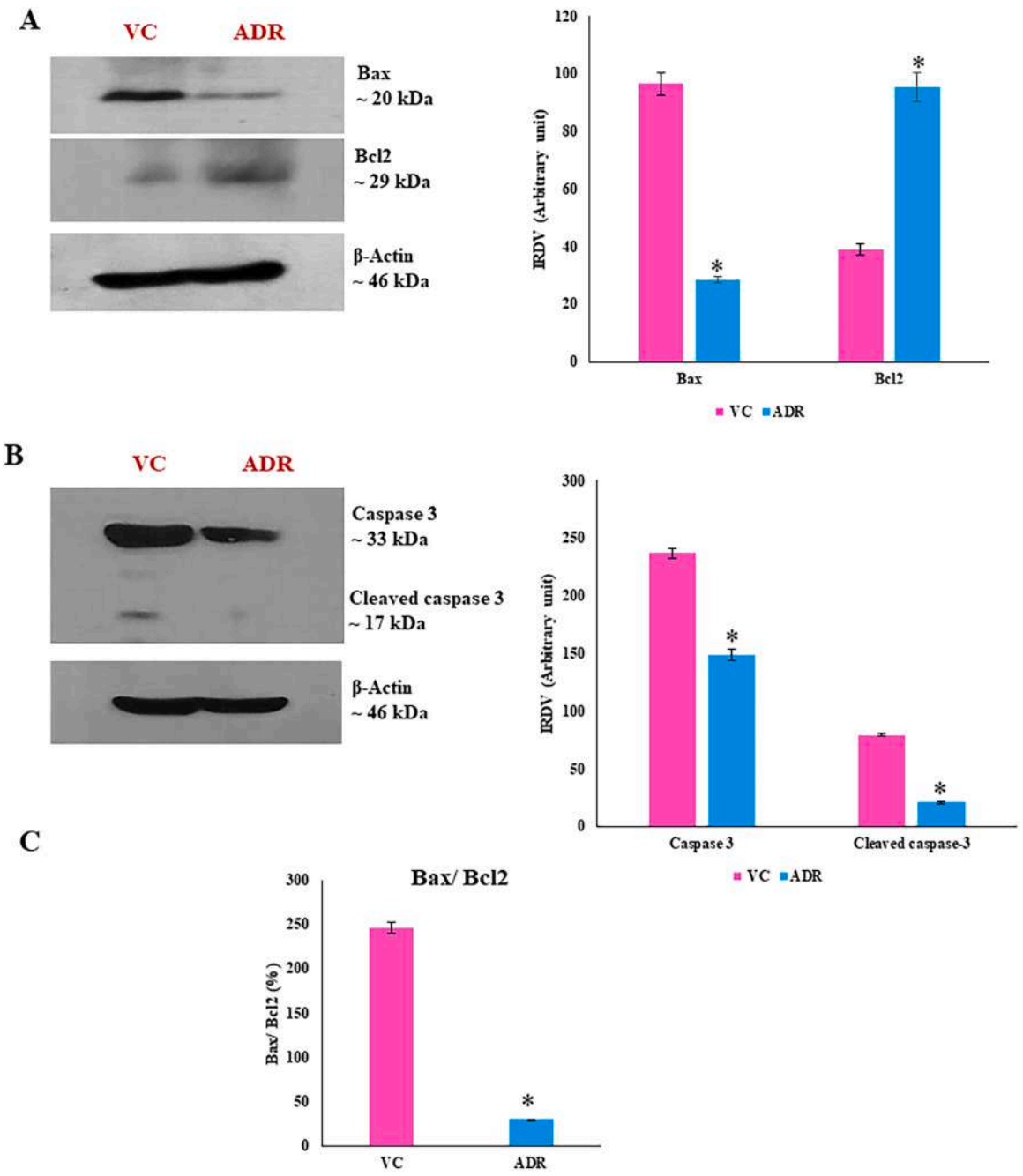

Fig. 9. Representative immunoblots and densitometric analysis of (A) BAX and BCL2, (B) Caspase 3 and cleaved caspase 3 proteins in VC and ADR group. (C) The bar graph shows the BAX/BCL2 ratio (in %) in the ovary of adropin-treated adult mice. Data are expressed as IRDV±SEM (n= 3), analyzed by unpaired t-test. A bar with a (*) superscript indicates a statistically significant ($p<0.05$) difference between the mean values of VC and ADR groups. VC, Vehicle control; ADR, adropin-treated (450 nmol/kg b.w.) group.

4. Discussion

The current study is an extension of our previous study in which we observed intense immunoreactivity of adropin and its putative receptor, GPR19, in corpus luteum, and *in vitro* treatment of adropin resulted into increased expression of markers associated with CL formation and its function [27]. This study explores the *in-vitro* effect of adropin on hCG-induced ovarian function, and the *in-vivo* effect of exogenous treatment of adropin on ovarian function was also evaluated with special emphasis on CL functions.

hCG is a well-known hormone that is involved in the maintenance of corpus luteum function, and in mice, it affects pituitary and ovarian hormones in a similar manner to that observed in humans [34]. So, in order to find out the role of adropin on hCG-induced ovarian function, an *in-vitro* study was performed in which ovaries were cultured with different concentrations of adropin (10,100 ng/ml adropin) along with hCG. Our result demonstrated that adropin, along with hCG, induces steroidogenesis markers StAR, 3β-HSD, and aromatase expression, leading to increased P4 and E2 synthesis, and it also decreases BAX/BCL2 ratio in mice ovary. These results clearly indicated that adropin acts synergistically with hCG to promote steroid hormone synthesis and survival of ovarian cells in mice. So, it would be quite interesting to observe the effect of adropin on corpus luteum survival and function in *in-vivo* system.

Table 2
Correlations between ovarian GPR19 protein expression with circulating P4, 3β-HSD, antioxidant proteins (SOD, catalase, NRF-2, HO-1, BCL2), LPO, and apoptotic proteins (BAX, cleaved caspase 3) in ADR mice ovary. p-value is the probability value, and r is Pearson's correlation coefficient.

Parameters	GPR19
Serum P4	r = 0.882* P< 0.05
3β-HSD	r = 0.967** P< 0.01
SOD	r = 0.988** P< 0.01
Catalase	r = 0.874* P< 0.05
LPO	r = −0.960** P< 0.01
NRF-2	r = 0.822* P< 0.05
HO-1	r = 0.954** P< 0.01
BCL2	r = 0.949** P< 0.01
BAX	r = −0.989** P< 0.01
Cleaved Caspase 3	r= −0.990** P< 0.01

In order to find out *in-vivo* effect of adropin on ovarian function, adult female mice were treated with adropin (450 nmol/kg b.w). First, we examined the effect of adropin on ovarian steroidogenesis. Adropin treatment resulted into a significant increase in StAR and 3β-HSD enzyme expression, while CYP11A1 and aromatase expression was decreased. So, adropin treatment resulted into increased P4 and decreased E2 synthesis. It is difficult to explain the discrepancy between increased P4 and decreased CYP11A1 expression. **Stocco et al., 2001** reported that LH-mediated decreased P4 production is due to decreased StAR and 3β-HSD, without affecting P_{450}SCC gene expression [35]. We gave adropin treatment at three-time points in single day. A longer duration of treatment may clarify the regulation of SCC protein expression by adropin. 3β-HSD enzyme converts pregnenolone into progesterone [36], while aromatase is responsible for the conversion of testosterone into estradiol [37]. These finding clearly indicate that adropin promotes P4 synthesis by elevating the expression of 3β-HSD while decreases E2 synthesis by inhibiting aromatase expression. CL is regarded as the main site for P4 synthesis [38], and various studies have reported that estrogen can shorten the luteal life span and stimulate the luteolytic pathway in various species, including rodents [39–41]. So, increased P4 and decreased E2 in adropin-treated mice ovary is indicative of its possible positive role in CL survival and maintenance. The differences in the effects of adropin on ovarian steroidogenesis may be due to the fact that adropin has a direct impact on the gonad when it is administered *in vitro,* whereas when it is administered *in vivo,* the effects may be mediated both indirectly through the hypothalamus-pituitary-ovary axis as well as directly on the ovary.

CL is a very active site for steroidogenesis and has intense vasculature, providing easy release of P4 directly into the circulation [42]. Because of the vast blood vessel network and steroidogenic activity, CL is considered to be highly susceptible to locally generated ROS [43], and ROS accumulation is associated with luteal regression [44–48]. So, in second part, we examined the effect of adropin on antioxidant potential of the mice ovary. Exogenous adropin treatment resulted into increased expression of GPR19, NRF-2, HO-1, and NF-κB along with increased SOD and catalase activity but decreased LPO in mice ovary. NRF-2 is a transcription factor and is a key sensor of oxidative stress [49]. Upon exposure of cells to oxidative stress, NRF-2 undergoes translocation to the nucleus and binds with the antioxidant response element (ARE), thereby facilitating the activation of phase II antioxidant enzymes and antioxidant proteins such as heme oxygenase 1 (HO-1), SOD (Superoxide dismutase), CAT (Catalase) [50,51]. SOD facilitates the dismutation of superoxides (O_2^-) into elemental oxygen and H_2O_2, thereby neutralizing free radicals [52], while CAT protects cells from H_2O_2 toxicity by breaking it down into H_2O [53]. Western blot and IF study clearly indicated increased expression and migration of NRF-2 in the nucleus of luteal cells in adropin treated mice ovary. Lipid peroxidation (LPO) is one of the consequences of oxidative stress, resulting in a loss of plasma membrane structure and functions [54]. The correlation study revealed a significant positive correlation of GPR19 with NRF-2, HO-1, SOD, and catalase, while LPO was found to be negatively correlated. Altogether, these findings clearly indicate that adropin promotes antioxidant potential by mediating the translocation of NRF-2 into the nucleus of luteal cells. Furthermore, we also observed significantly decreased BAX/BCL2 ratio, caspase 3, active caspase 3 expression, and TUNEL-positive luteal cells in adropin-treated mice ovary. Interestingly, the Western blot study revealed the increased expression of NF-κB, but the IF study clearly confirmed the decreased localization of NF-κB in the luteal cell nucleus of adropin-treated mice ovary. NF-κB is a redox-sensitive transcription factor that shows biphasic or bidirectional regulation by ROS [55]. It plays an important role in the regulation of immune responses, placental development, cellular growth and proliferation, apoptosis, and survival [56,57]. According to studies, rapid and early activation of NF-κB is advantageous for cells to combat ROS by reinforcing survival signals. While sustained, continuous activation of NF-κB results in apoptosis [55]. According to Kabe Y et al., 2005, ROS stimulates the NF-κB pathway by translocating it from the cytoplasm to the nucleus [58], and ROS-mediated apoptosis has been reported to be fundamental in determining the CL lifespan across various mammalian species [6,59–61]. Overall, these findings clearly demonstrated that adropin inhibits oxidative stress by promoting anti-oxidant enzyme activity via NRF-2 mediated pathway, and decreased oxidative stress inhibited the translocation of NF-κB into the luteal cell nucleus, resulting in increased survival and decreased apoptosis of luteal cells.

5. Conclusion

In conclusion, *in-vitro* results confirmed that adropin acts synergistically with hCG and upregulates steroidogenesis (E2 & P4) and ovarian cell survival by increasing the expression of StAR, CYP11A1, 3β-HSD, aromatase, and decreasing BAX/BCL2 ratio. Exogenous treatment of adropin enhances P4 production by increasing the expression of StAR, 3β-HSD. Adropin treatment reduces oxidative stress by increasing the antioxidant proteins and enzymes, including NRF-2, HO-1, BCL2, SOD, and catalase. Adropin also inhibits the nuclear translocation of NF-κB, that may result into decreased BAX/BCL2 ratio, caspase 3 & active caspase 3 expression, and TUNEL-positive cells, resulting into decreased luteal cell apoptosis. Overall, this provides a novel viewpoint that adropin can be an interesting candidate that can enhance the survivability of the CL. (Fig. 10).

Funding

This work was funded by DST- SERB (File no. ECR/2016/001883/LS), New Delhi, India.

CRediT authorship contribution statement

Taruna Arora: Writing – review & editing, Investigation, Conceptualization. **AJIT SINGH:** Writing – review & editing, Supervision, Resources, Project administration, Investigation, Funding acquisition, Conceptualization. **Shweta Maurya:** Writing – review & editing, Writing – original draft, Validation, Methodology, Investigation, Conceptualization. **Shashank Tripathi:** Writing – review & editing, Validation, Methodology, Formal analysis, Conceptualization.

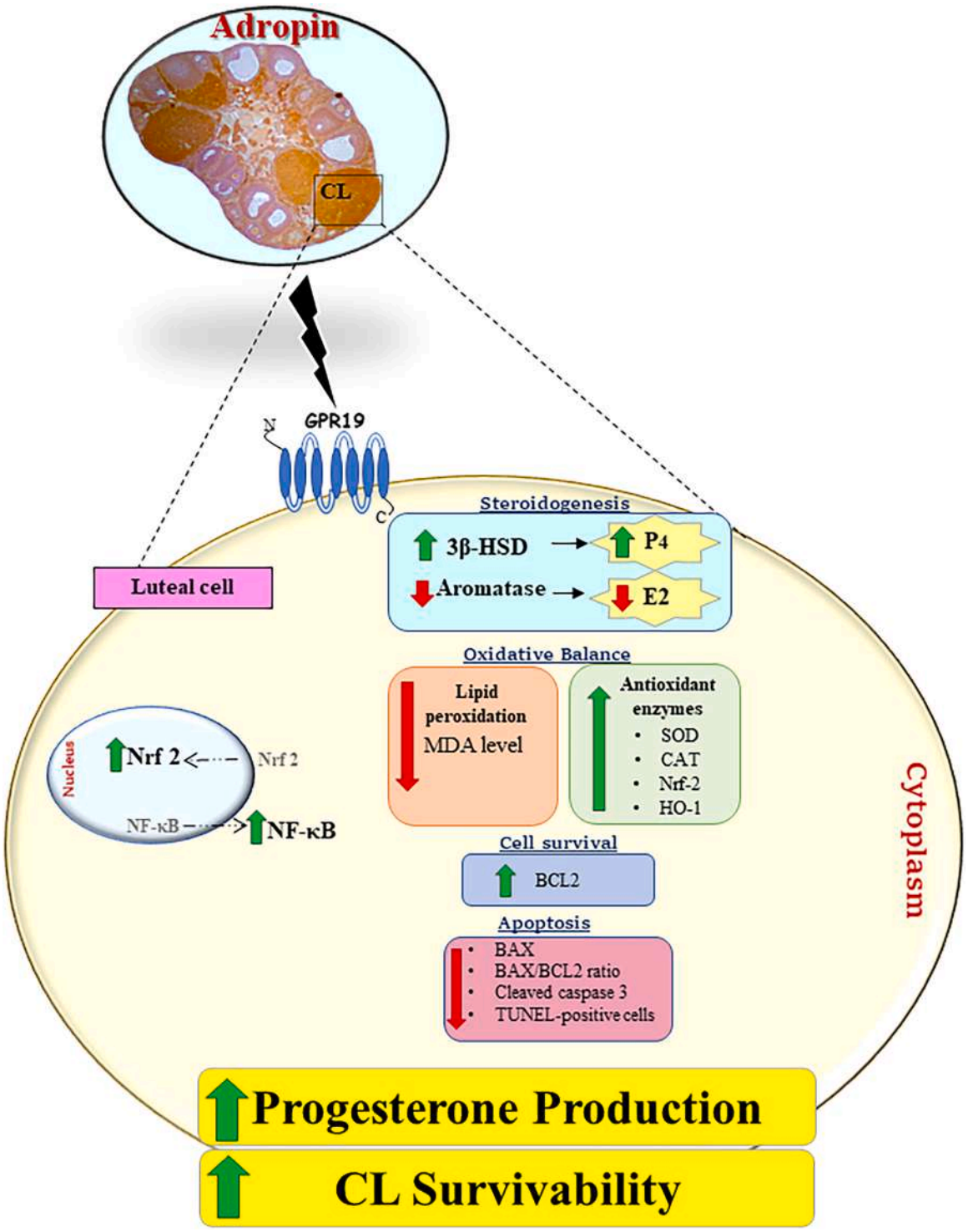

Fig. 10. Schematic diagram showing the potential involvement of adropin in the ovarian functions of adult mice. Exogenous adropin administration in adult mice enhances progesterone production by increasing the expression of StAR, 3β-HSD but reduces estradiol by decreasing aromatase expression in the ovary. Additionally, adropin also promotes the expression and activity of antioxidant proteins and enzymes such as NRF-2, HO-1, SOD, and catalase. Decreased oxidative stress may result in decreased translocation of NF-κB into the nucleus of luteal cells, resulting into decreased lipid peroxidation, BAX/BCL2 ratio, caspase 3, active caspase3 expression, and TUNEL-positive luteal cells in adropin treated mice. Overall, adropin can be an interesting candidate that could enhance CL survivability.

Declaration of Competing interest

The authors declare that there are no conflicts of interest.

Data availability

Data will be made available on request.

Acknowledgments

Shweta Maurya and Shashank Tripathi are thankful to CSIR, New Delhi, for the award of Junior and Senior research fellowship. DST-FIST and UGC-CAS program to the Department of Zoology, BHU, is acknowledged. The authors are thankful to Sophisticated Analytical and Technical Help Institute (SATHI), BHU, India, for providing a laser scanning super-resolution microscope facility.

References

[1] I. Hanukoglu, Antioxidant protective mechanisms against reactive oxygen species (ROS) generated by mitochondrial P450 systems in steroidogenic cells, Drug Metab. Rev. 38 (1-2) (2006) 196, https://doi.org/10.1080/03602530600570040.
[2] J.D. Wardyn, A.H. Ponsford, C.M. Sanderson, Dissecting molecular cross-talk between Nrf2 and NF-κB response pathways, Biochem Soc. Trans. 43 (4) (2015) 621–626, https://doi.org/10.1042/BST20150014.
[3] J. Lim, L. Ortiz, B.N. Nakamura, Y.D. Hoang, J. Banuelos, V.N. Flores, et al., Effects of deletion of the transcription factor Nrf2 and benzo[a]pyrene treatment on ovarian follicles and ovarian surface epithelial cells in mice, Reprod. Toxicol. 58 (2015) 24–32, https://doi.org/10.1016/j.reprotox.2015.07.080.
[4] X. Luo, J. Xu, R. Zhao, J. Qin, X. Wang, Y. Yan, et al., The role of inactivated NF-κB in premature ovarian failure, Am. J. Pathol. 192 (3) (2022) 468–483, https://doi.org/10.1016/j.ajpath.2021.12.005.
[5] A. Agarwal, S. Gupta, S. Sikka, The role of free radicals and antioxidants in reproduction, Curr. Opin. Obstet. Gynecol. 18 (3) (2006) 325–332, https://doi.org/10.1097/01.gco.0000193003.58158.4e.
[6] H.R. Behrman, P.H. Kodaman, S.L. Preston, S. Gao, Oxidative stress and the ovary (Suppl Proceedings), J. Soc. Gynecol. Invest. 8 (1) (2001) S40–2, https://doi.org/10.1016/s1071-5576(00)00106-4.
[7] A. Agarwal, S.S.R. Allamaneni, Role of free radicals in female reproductive diseases and assisted reproduction, Reprod. Biomed. Online 9 (3) (2004) 338–347, https://doi.org/10.1016/s1472-6483(10)62151-7.
[8] S. Gupta, A. Agarwal, J. Banerjee, J.G. Alvarez, The role of oxidative stress in spontaneous abortion and recurrent pregnancy loss: a systematic review, quiz 353, Obstet. Gynecol. Surv. 62 (5) (2007) 335–347, https://doi.org/10.1097/01.ogx.0000261644.89300.df.
[9] S. Gupta, A. Agarwal, N. Krajcir, J.G. Alvarez, Role of oxidative stress in endometriosis, Reprod. Biomed. Online 13 (1) (2006) 126–134, https://doi.org/10.1016/s1472-6483(10)62026-3.
[10] S.D. Shukla, M. Bhatnagar, S. Khurana, Critical evaluation of ayurvedic plants for stimulating intrinsic antioxidant response, Front Neurosci. 6 (2012) 112, https://doi.org/10.3389/fnins.2012.00112.
[11] K.G. Kumar, J.L. Trevaskis, D.D. Lam, G.M. Sutton, R.A. Koza, V.N. Chouljenko, et al., Identification of adropin as a secreted factor linking dietary macronutrient intake with energy homeostasis and lipid metabolism, Cell Metab. 8 (6) (2008) 468–481, https://doi.org/10.1016/j.cmet.2008.10.011.
[12] K.G. Kumar, J. Zhang, S. Gao, J. Rossi, O.P. McGuinness, H.H. Halem, et al., Adropin deficiency is associated with increased adiposity and insulin resistance, Obes. (Silver Spring) 20 (7) (2012) 1394–1402, https://doi.org/10.1038/oby.2012.31.
[13] S. Yosaee, M. Khodadost, A. Esteghamati, J.R. Speakman, F. Shidfar, M.N. Nazari, et al., Metabolic syndrome patients have lower levels of adropin when compared with healthy overweight/obese and lean subjects, Am. J. Mens. Health 11 (2) (2017) 426–434, https://doi.org/10.1177/1557988316664074.
[14] A.A. Butler, C.S. Tam, K.L. Stanhope, B.M. Wolfe, M.R. Ali, M. O'Keeffe, et al., Low circulating adropin concentrations with obesity and aging correlate with risk factors for metabolic disease and increase after gastric bypass surgery in humans, J. Clin. Endocrinol. Metab. 97 (10) (2012) 3783–3791, https://doi.org/10.1210/jc.2012-2194.
[15] S. Gao, S. Ghoshal, L. Zhang, J.R. Stevens, K.S. McCommis, B.N. Finck, et al., The peptide hormone adropin regulates signal transduction pathways controlling hepatic glucose metabolism in a mouse model of diet-induced obesity, J. Biol. Chem. 294 (36) (2019) 13366–13377, https://doi.org/10.1074/jbc.RA119.008967.
[16] S. Gao, R.P. McMillan, J. Jacas, Q. Zhu, X. Li, K.G. Kumar, et al., Regulation of substrate oxidation preferences in muscle by the peptide hormone adropin, Diabetes 63 (10) (2014) 3242–3252, https://doi.org/10.2337/db14-0388.
[17] M. Jasaszwili, T. Wojciechowicz, M. Billert, M.Z. Strowski, K.W. Nowak, M. Skrzypski, Effects of adropin on proliferation and differentiation of 3T3-L1 cells and rat primary preadipocytes, Mol. Cell Endocrinol. 496 (2019) 110532, https://doi.org/10.1016/j.mce.2019.110532.
[18] F. Lovren, Y. Pan, A. Quan, K.K. Singh, P.C. Shukla, M. Gupta, et al., Adropin is a novel regulator of endothelial function (Suppl:), Circulation 122 (11) (2010) S185–92, https://doi.org/10.1161/CIRCULATIONAHA.109.931782.
[19] M. Topuz, A. Celik, T. Aslantas, A.K. Demir, S. Aydin, S. Aydin, Plasma adropin levels predict endothelial dysfunction like flow-mediated dilatation in patients with type 2 diabetes mellitus, J. Invest. Med 61 (8) (2013) 1161–1164, https://doi.org/10.2310/JIM.0000000000000003.
[20] T.R. Altamimi, S. Gao, Q.G. Karwi, A. Fukushima, S. Rawat, C.S. Wagg, et al., Adropin regulates cardiac energy metabolism and improves cardiac function and efficiency, Metabolism 98 (2019) 37–48, https://doi.org/10.1016/j.metabol.2019.06.005.
[21] S. Tripathi, S. Maurya, A. Singh, Adropin may promote insulin stimulated steroidogenesis and spermatogenesis in adult mice testes, J. Exp. Zool. A Ecol. Integr. Physiol. (2023), https://doi.org/10.1002/jez.2763.
[22] X. Chen, H. Xue, W. Fang, K. Chen, S. Chen, W. Yang, et al., Adropin protects against liver injury in nonalcoholic steatohepatitis via the Nrf2 mediated antioxidant capacity, Redox Biol. 21 (2019) 101068, https://doi.org/10.1016/j.redox.2018.101068.
[23] A. Singh, P. Bora, A. Krishna, Direct action of adiponectin ameliorates increased androgen synthesis and reduces insulin receptor expression in the polycystic ovary, Biochem Biophys. Res Commun. 488 (3) (2017) 509–515, https://doi.org/10.1016/j.bbrc.2017.05.076.
[24] A. Singh, M. Choubey, P. Bora, A. Krishna, Adiponectin and chemerin: contrary Adipokines in regulating reproduction and metabolic disorders, Reprod. Sci. 25 (10) (2018) 1462–1473, https://doi.org/10.1177/1933719118770547.
[25] A. Estienne, A. Bongrani, M. Reverchon, C. Ramé, P.H. Ducluzeau, P. Froment, J. Dupont, Involvement of novel Adipokines, chemerin, visfatin, resistin and apelin in reproductive functions in normal and pathological conditions in humans and animal models, Int J. Mol. Sci. 20 (18) (2019) 4431, https://doi.org/10.3390/ijms20184431.
[26] K. Sato, T. Yamashita, R. Shirai, K. Shibata, T. Okano, M. Yamaguchi, et al., Adropin contributes to anti-atherosclerosis by suppressing monocyte-endothelial cell adhesion and smooth muscle cell proliferation, Int J. Mol. Sci. 19 (5) (2018) 1293, https://doi.org/10.3390/ijms19051293.
[27] S. Maurya, S. Tripathi, T. Arora, A. Singh, Adropin may regulate corpus luteum formation and its function in adult mouse ovary, Horm. (Athens) 22 (4) (2023) 725–739, https://doi.org/10.1007/s42000-023-00476-0.
[28] S. Maurya, S. Tripathi, A. Singh, Ontogeny of adropin and its receptor expression during postnatal development and its pro-gonadal role in the ovary of pre-pubertal mouse, J. Steroid Biochem Mol. Biol. 234 (2023) 106404, https://doi.org/10.1016/j.jsbmb.2023.106404.
[29] S. Maurya, A. Singh, Asprosin modulates testicular functions during ageing in mice, Gen. Comp. Endocrinol. 323-324 (2022) 114036, https://doi.org/10.1016/j.ygcen.2022.114036.
[30] M.M. Bradford, A rapid and sensitive method for the quantitation of microgram quantities of protein utilizing the principle of protein-dye binding, Anal. Biochem 72 (1-2) (1976) 248–254, https://doi.org/10.1006/abio.1976.9999.
[31] K. Das, L. Samanta, N.B.G. Chainy, A modified spectrophotometric assay of superoxide dismutase using nitrite formation by superoxide radicals, Ind. J. Biochem Biophys. 37 (2000) 201–204.
[32] A.K. Sinha, Colorimetric assay of catalase, Anal. Biochem 47 (2) (1972) 389–394, https://doi.org/10.1016/0003-2697(72)90132-7.
[33] H. Ohkawa, N. Ohishi, K. Yagi, Reaction of linoleic acid hydroperoxide with thiobarbuteric acid. J. Lipid Res 19 (8) (1978) 1053–1057, https://doi.org/10.1016/S0022-2275(20)40690-X.
[34] M.M. Al-Shebaily, Evaluation of the effects of Pregnyl on pituitary-ovarian hormones and biochemical markers of tissue injury in female Swiss albino mice, Res Commun. Mol. Pathol. Pharm. 105 (1-2) (1999) 155–171.
[35] C.O. Stocco, J. Chedrese, R.P. Deis, Luteal expression of cytochrome P450 side-chain cleavage, steroidogenic acute regulatory protein, 3beta-hydroxysteroid dehydrogenase, and 20alpha-hydroxysteroid dehydrogenase genes in late pregnant rats: effect of luteinizing hormone and RU486, Biology of reproduction 65 (4) (2001) 1114–1119. https://doi.org/10.1095/biolreprod65.4.1114.
[36] J.C. Chapman, J.R. Polanco, S. Min, S.D. Michael, Mitochondrial 3 beta-hydroxysteroid dehydrogenase (HSD) is essential for the synthesis of progesterone by corpora lutea: an hypothesis, Reprod. Biol. Endocrinol. 3 (1) (2005) 11, https://doi.org/10.1186/1477-7827-3-11.
[37] C. Stocco, Aromatase expression in the ovary: hormonal and molecular regulation, Steroids 73 (5) (2008) 473–487, https://doi.org/10.1016/j.steroids.2008.01.017.
[38] C. Stocco, C. Telleria, G. Gibori, The molecular control of corpus luteum formation, function, and regression, Endocr. Rev. 28 (1) (2007) 117–149, https://doi.org/10.1210/er.2006-0022.
[39] F.J. Karsch, G.P. Sutton, An intra-ovarian site for the luteolytic action of estrogen in the rhesus monkey, Endocrinology 98 (1976) 553–561, https://doi.org/10.1210/endo-98-3-553.
[40] J.N. Schoonmaker, W. Victery, F.J. Karsch, A receptive period for estradiol-induced luteolysis in the rhesus monkey, Endocrinology 108 (1981) 1874–1877, https://doi.org/10.1210/endo-108-5-1874.
[41] S. Plas-Roser, B. Muller, C. Aron, Estradiol involvement in the luteolytic action of LH during the estrous cycle in the rat, Exp. Clin. Endocrinol. 92 (2) (1988) 145–153.
[42] L.P. Reynolds, A.T. Grazul-Bilska, D.A. Redmer, Angiogenesis in the corpus luteum, Endocrine 12 (1) (2000) 1–9, https://doi.org/10.1385/ENDO:12:1:1.
[43] K.H. Al-Gubory, C. Garrel, P. Faure, N. Sugino, Roles of antioxidant enzymes in corpus luteum rescue from reactive oxygen species-induced oxidative stress,

Reprod. Biomed. Online 25 (6) (2012) 551–560, https://doi.org/10.1016/j.rbmo.2012.08.004.
[44] H.R. Behrman, R.F. Aten, Evidence that hydrogen peroxide blocks hormone-sensitive cholesterol transport into mitochondria of rat luteal cells, Endocrinology 128 (6) (1991) 2958–2966, https://doi.org/10.1210/endo-128-6-2958.
[45] E. Gatzuli, R.F. Aten, H.R. Behrman, Inhibition of gondatropic action and progesterone synthesis by xanthine oxidase in rat luteal cells, Endocrinology 128 (5) (1991) 2253–2258, https://doi.org/10.1210/endo-128-5-2253.
[46] B. Musicki, R.F. Aten, H.R. Behrman, Inhibition of protein synthesis and hormone-sensitive steroidogenesis in response to hydrogen peroxide in rat luteal cells, Endocrinology 134 (2) (1994) 588–595, https://doi.org/10.1210/endo.134.2.7507829.
[47] J.C.M. Riley, H.R. Behrman, In vivo generation of hydrogen peroxide in the rat corpus luteum during luteolysis, Endocrinology 128 (4) (1991) 1749–1753, https://doi.org/10.1210/endo-128-4-1749.
[48] M. Sawada, J.C. Carlson, Superoxide radical production in plasma membrane samples from regressing rat corpora lutea, Can. J. Physiol. Pharm. 67 (5) (1989) 465–471, https://doi.org/10.1139/y89-074.
[49] M. Zhang, C. An, Y. Gao, R.K. Leak, J. Chen, F. Zhang, Emerging roles of Nrf2 and phase II antioxidant enzymes in neuroprotection, Prog. Neurobiol. 100 (2013) 30–47, https://doi.org/10.1016/j.pneurobio.2012.09.003.
[50] Q. Ma, Role of nrf2 in oxidative stress and toxicity, Annu Rev. Pharm. Toxicol. 53 (2013) 401–426, https://doi.org/10.1146/annurev-pharmtox-011112-140320.
[51] N. Keleku-Lukwete, M. Suzuki, M. Yamamoto, An overview of the advantages of KEAP1-NRF2 system activation during inflammatory disease treatment, Antioxid. Redox Signal 29 (17) (2018) 1746–1755, https://doi.org/10.1089/ars.2017.7358.
[52] Y. Wang, R. Branicky, A. Noë, S. Hekimi, Superoxide dismutases: dual roles in controlling ROS damage and regulating ROS signaling, J. Cell Biol. 217 (6) (2018) 1915–1928, https://doi.org/10.1083/jcb.201708007.
[53] S. Wang, G. He, M. Chen, T. Zuo, W. Xu, X. Liu, The role of antioxidant enzymes in the ovaries, Oxid. Med Cell Longev. (2017) 4371714, https://doi.org/10.1155/2017/4371714.
[54] A. Ayala, M.F. Muñoz, S. Argüelles, Lipid peroxidation: production, metabolism, and signaling mechanisms of malondialdehyde and 4-hydroxy-2-nonenal, Oxid. Med Cell Longev. (2014) 360438, https://doi.org/10.1155/2014/360438.
[55] S. Nakajima, M. Kitamura, Bidirectional regulation of NF-kappaB by reactive oxygen species: a role of unfolded protein response, Free Radic. Biol. Med 65 (2013) 162–174, https://doi.org/10.1016/j.freeradbiomed.2013.06.020.
[56] M.J. Morgan, Z.G. Liu, Crosstalk of reactive oxygen species and NF-κB signaling, Cell Res 21 (1) (2011) 103–115, https://doi.org/10.1038/cr.2010.178.
[57] B. Armistead, L. Kadam, S. Drewlo, H.R. Kohan-Ghadr, The role of NFκB in healthy and preeclamptic placenta: trophoblasts in the spotlight, Int J. Mol. Sci. 21 (5) (2020) 1775, https://doi.org/10.3390/ijms21051775.
[58] Y. Kabe, K. Ando, S. Hirao, M. Yoshida, H. Handa, Redox regulation of NF-kappaB activation: distinct redox regulation between the cytoplasm and the nucleus, Antioxid. Redox Signal 7 (3-4) (2005) 395–403, https://doi.org/10.1089/ars.2005.7.395.
[59] C. Garrel, I. Ceballos-Picot, G. Germain, K.H. Al-Gubory, Oxidative stress-inducible antioxidant adaptive response during prostaglandin F2alpha-induced luteal cell death in vivo, Free Radic. Res 41 (3) (2007) 251–259, https://doi.org/10.1080/10715760601067493.
[60] H. Kato, N. Sugino, S. Takiguchi, S. Kashida, Y. Nakamura, Roles of reactive oxygen species in the regulation of luteal function, Rev. Reprod. 2 (2) (1997) 81–83, https://doi.org/10.1530/ror.0.0020081.
[61] M. Tanaka, T. Miyazaki, S. Tanigaki, K. Kasai, K. Minegishi, K. Miyakoshi, et al., Participation of reactive oxygen species in PGF2alpha-induced apoptosis in rat luteal cells, J. Reprod. Fertil. 120 (2) (2000) 239–245, https://doi.org/10.1530/jrf.0.1200239.